EPR linewidths in $La_{1-x}Ca_xMnO_3$: $0 \leqslant x \leqslant 1$

D. L. Huber
Department of Physics, University of Wisconsin–Madison, Madison, Wisconsin 53706

G. Alejandro, A. Caneiro, M. T. Causa, F. Prado, and M. Tovar
Centro Atómico Bariloche and Instituto Balseiro, Comisión Nacional de Energía Atómica and Universidad Nacional de Cuyo, 8400 San Carlos de Bariloche, Río Negro, Argentina

S. B. Oseroff
San Diego State University, San Diego, California 92182
(Received 27 January 1999)

We have analyzed recent results for the electron paramagnetic resonance linewidths in $La_{1-x}Ca_xMnO_3$ and related materials over the range $0 \leqslant x \leqslant 1$. In all cases studied, the linewidth away from magnetic and structural transitions can be fitted to the expression $[\chi_0(T)/\chi(T)]\Delta H_{\text{p.p.}}(\infty)$, where the first factor is the ratio of the Curie susceptibility $\chi_0(T)$ to the measured susceptibility $\chi(T)$ and the second factor is a temperature-independent constant. Formally exact and approximate expressions for $\Delta H_{\text{p.p.}}(\infty)$ are derived. In the case of $LaMnO_3$, the linewidth in the distorted O′ phase arises from the interplay of crystal field (single ion) anisotropy and antisymmetric (Dzialozhinsky-Moriya) exchange together with isotropic superexchange. Above the Jahn-Teller transition to the pseudocubic O phase, the single-ion anisotropy is much weaker and the linewidth arises primarily from the antisymmetric interactions. Similar behavior is also found in both phases of the less-distorted, oxygenated material $LaMnO_{3.04}$. In the case of $CaMnO_3$, the distortions of the oxygen octahedra are also small and the antisymmetric interactions are again dominant. In the intermediate region $0<x<1$, $\Delta H_{\text{p.p.}}(\infty)$ decreases with increasing Ca (i.e., Mn^{4+}) concentration in contrast to the Curie-Weiss temperature, which peaks near $x=1/3$, reflecting the importance of the double-exchange mechanism. It is proposed that the absence of a signature of the double-exchange interaction in the infinite-temperature linewidth is a consequence of the fact that the time scale associated with the changes in Mn valence arising from double exchange is too long to affect the decay of the correlation function in $\Delta H_{\text{p.p.}}(\infty)$ so that the linewidth is determined primarily by the superexchange interactions between the Mn ions. [S0163-1829(99)08841-9]

I. INTRODUCTION

In recent years, lanthanum-based manganites with the general formula $La_{1-x}A_xMnO_3$ and perovskite structure have been extensively studied both for their intrinsic interest and because of possible applications in magnetic recording. The latter comes about because of the *colossal* magnetoresistance (CMR) that appears when a fraction of the trivalent lanthanum ions are replaced by divalent impurities such as Ca or Sr. The high values for the magnetoresistance are associated with mobile e_g electrons that introduce ferromagnetic correlations between the spins through the mechanism of double exchange.[1–5] The double-exchange interaction is in addition to the conventional superexchange coupling between fixed (immobile) spins. It should be noted that similar effects have also been observed in $LaMnO_{3+\delta}$.[6]

In studying the magnetic properties of these materials, it is important to investigate the dynamics of the spins as well as their static properties, especially because the double-exchange mechanism is an intrinsically dynamical process. There are two direct experimental probes of spin dynamics: magnetic resonance and inelastic neutron scattering. While neutron scattering has provided much information about the magnetically ordered phases of the manganites, it has had limited use in probing the dynamics of the paramagnetic region. In contrast, electron paramagnetic resonance (EPR) measurements have been carried out in a variety of samples over a wide temperature range.[7]

In the EPR measurements, the parameters of primary interest are the g factors and the linewidths. In the case of the manganites, the g factors are nearly temperature independent (except possibly very close to ferromagnetic phase transitions) and very nearly equal to the free electron value. In contrast, the linewidths show a wide variety of behaviors depending on both the temperature and concentration of divalent ions. Outside the critical regions associated with the magnetic and structural transitions, however, the temperature dependence of the linewidths of many of the manganites has been found to be described by the simple formula

$$\Delta H(T)=[\chi_0(T)/\chi(T)]\Delta H(\infty), \tag{1}$$

where $\Delta H(T)$ denotes the linewidth at temperature T, $\chi_0(T)$ is the free spin (Curie) susceptibility $[\chi_0(T) \propto T^{-1}]$, and $\chi(T)$ is the measured susceptibility. The symbol $\Delta H(\infty)$ is a temperature-independent constant. Since $\chi(T) \rightarrow \chi_0(T)$ as $T \rightarrow \infty$, $\Delta H(\infty)$ is identified with the high-temperature limit of the linewidth. Although $\Delta H(\infty)$ is temperature independent, it does depend on the concentration of divalent ions and the structural phase of the material.

In Fig. 1, we summarize the results of recent measurements of the peak-to-peak linewidth $\Delta H_{\text{p.p.}}(\infty)$ in the

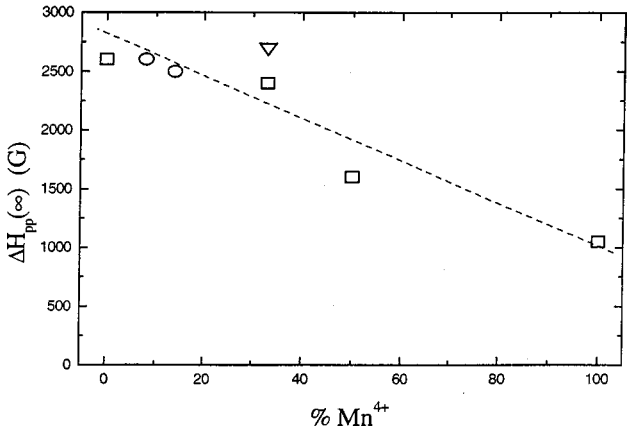

FIG. 1. $\Delta H_{\mathrm{p.p.}}(\infty)$ vs % Mn^{4+} content for various manganite compounds: (□) $La_{1-x}Ca_xMnO_3$, (▽) $La_{0.77}Sr_{0.33}MnO_3$, and (○) $LaMnO_{3+\delta}$. In the case of $LaMnO_3$, the linewidth refers to the high-temperature O phase. The dashed line is a guide to the eye.

calcium-doped material $La_{1-x}Ca_xMnO_3$. In this figure, $\Delta H_{\mathrm{p.p.}}(\infty)$ is plotted against the Mn^{4+} content. The value for $x=0$ is the linewidth in the pseudocubic O phase. The dashed line, drawn as a guide to the eye, shows the overall trend in the variation of the linewidth with Mn^{4+} concentration. From the figure, it is evident that the value of $\Delta H_{\mathrm{p.p.}}(\infty)$ for $x=0.33$, which corresponds to the highest value of the ferromagnetic ordering temperature, is quite close to the values in the undoped material, which orders antiferromagnetically. For comparison, we also show the values of $\Delta H_{\mathrm{p.p.}}(\infty)$ for $LaMnO_{3+\delta}$ and $La_{0.7}Sr_{0.3}MnO_3$. The corresponding numerical values of the linewidth are given in Table I.

In this paper, we will analyze and interpret the data for $\Delta H(\infty)$. We will show how Eq. (1) arises naturally from a consideration of the dynamics of the fluctuations of the total spin in an exchange-coupled system. We will demonstrate how the different values of $\Delta H(\infty)$ in the O and O′ phases reflect the comparative importance of various anisotropy mechanisms. We will also show that the values of $\Delta H(\infty)$ for $x=0.33$ and 0.50 provide limits on the time scale of the polaron dynamics associated with the e_g electrons.

The organization of the paper is as follows. Section II is devoted to an outline of the relevant theory. In Sec. III, we analyze the results for the $LaMnO_3$ and $CaMnO_3$, while in Sec. IV, we consider the behavior of $La_{1-x}Ca_xMnO_3$ for $0<x<1$. Section V contains a discussion of our findings.

TABLE I. $\Delta H_{\mathrm{pp}}(\infty)$ and Curie-Weiss temperature for samples with different percentage of Mn^{4+}.

Compound	% Mn^{4+}	$\Delta H_{\mathrm{p.p.}}(\infty)$ (G)	Θ_{cw} (K)	
$LaMnO_3$	0	2600	220	Ref. 10
$LaMnO_{3.04}$	8	2600	210	This work
$LaMnO_{3.07}$	14	2500	250	This work
$La_{0.67}Ca_{0.33}MnO_3$	33	2400	370	Ref. 7
$La_{0.67}Sr_{0.33}MnO_3$	33	2700	470	Ref. 7
$La_{0.5}Ca_{0.5}MnO_3$	50	1600	250	This work
$CaMnO_3$	100	1050	350	Ref. 21 and this work

II. THEORY

In order to see how the exchange narrowing comes about, we use a general expression for relaxation rate of the total spin given previously in an analysis of electron paramagnetic resonance in systems with unlike spins.[8] In this approach, which is based on the memory function formalism developed by Mori,[9] the relaxation rate of the transverse (to the applied field) components S^+ and S^- of the total spin, or $1/T_2$, is given by the expression

$$1/T_2=(S^+,S^-)^{-1}\int_0^\infty dt e^{-i\omega_0 t}\times\left(\exp[it(1-P)L](1-P)\frac{dS^+}{dt},(1-P)\frac{dS^-}{dt}\right). \tag{2}$$

In this equation, ω_0 denotes the resonance frequency, P is a projection operator onto the low frequency modes,[9] and L is the Liouville operator with the property

$$A(t)=\exp[itL]A(0). \tag{3}$$

The symbol (A,B) denotes the susceptibility (or Kubo) inner product defined by

$$(A,B)=\int_0^\beta d\lambda\langle e^{\lambda H}Ae^{-\lambda H}B\rangle_T-\beta\langle A\rangle_T\langle B\rangle_T, \tag{4}$$

where $\beta=1/kT$ and the angular brackets denote a thermal average. Except very close to the ferromagnetic transition, where the magnetic properties are strongly affected by the applied field, we can usually evaluate Eq. (2) in the zero-field limit. At the same level of approximation, the projection operator can be eliminated leaving an expression of the form[8]

$$1/T_2\approx(S^+,S^-)^{-1}\int_0^\infty dt\left(\frac{dS^+(t)}{dt},\frac{dS^-(0)}{dt}\right). \tag{5a}$$

Since the integrand is an even function of t, the range of integration can be extended to $-\infty$, at which point the above integral can be rewritten as $(2kT)^{-1}$ times the integral of the thermal average of the symmetrized product $\{AB\}=\frac{1}{2}(AB+BA)$:[9]

$$1/T_2\approx\frac{1}{2kT(S^+,S^-)}\int_{-\infty}^{+\infty}dt\left\langle\left\{\frac{dS^+(t)}{dt}\frac{dS^-(0)}{dt}\right\}\right\rangle_T. \tag{5b}$$

In the standard Heisenberg picture, the time derivatives in Eq. (5b) can be expressed in terms of the commutators of the total spin with the Hamiltonian, i.e., $[S^+,H]$ and $[S^-,H]$. In the zero-field limit we can divide the Hamiltonian into isotropic (e.g., Heisenberg) and anisotropic parts H_{iso} and H_{anis}, respectively. The former, which are assumed to be dominant, are invariant under simultaneous rotation of all of the spins. As a consequence, the isotropic part of the Hamiltonian commutes with S^+ and S^-, so that Eq. (5b) becomes

$$1/T_2 = \frac{1}{4kT\chi(T)\hbar^2}\int_{-\infty}^{+\infty} dt \times \langle\{[S^+, H_{\text{anis}}](t)[H_{\text{anis}}, S^-](0)\}\rangle_T. \quad (6)$$

Here we have identified (S^+, S^-) with $2\chi(T), \chi(T)$ being the isothermal, zero-field susceptibility, which we have taken to be isotropic. Consistent with the assumption $H_{\text{iso}} \gg H_{\text{anis}}$, the time evolution of the correlation function in Eq. (6) is to be calculated with H_{iso} in place of H. The exchange narrowing comes about because $[S^+, H_{\text{anis}}]$ does not commute with the isotropic part of the Hamiltonian. As a result, the integral decays rapidly, with a time scale set by the dominant isotropic interaction. The EPR linewidth is thus much narrower than would be the case if there were no isotropic spin-spin interactions and the linewidth was expressed simply as the rms anisotropy field. In the Appendix to this paper, we make the connection between Eq. (6) and the more familiar form for the linewidth that involves the spectral moments of the line shape function. It should be noted that Eq. (6) can also be obtained from the self-energy of the Greens function associated with the operators S^+ and S^-.

As emphasized in the Introduction, the EPR linewidth varies as $[T\chi(T)]^{-1}$ over a wide temperature range. From Eq. (6), it is evident that such behavior will arise when the integral of the symmetrized correlation function appearing in Eq. (6) is approximately temperature independent. This will happen if a majority of the eigenstates of H_{iso} which contribute significantly to the integral all have energies that are much less than kT. Assuming this to be the case, we can express the parameter $\Delta H(\infty)$ appearing in Eq. (1) directly in terms of the integral. Noting that the peak-to-peak linewidth is equal to $(2/3^{1/2})\hbar(g\mu_B T_2)^{-1}$, we have

$$\Delta H_{\text{p.p.}}(\infty) = \frac{1}{2\sqrt{3}g\mu_B kC\hbar}\int_{-\infty}^{+\infty} dt \times \langle\{[S^+, H_{\text{anis}}](t)[H_{\text{anis}}, S^-](0)\}\rangle_\infty, \quad (7)$$

where C denotes the Curie constant [i.e., $\chi_0(T) = C/T$] and the integral is to be evaluated in the high-temperature limit.

In the Appendix, an approximate expression for $\Delta H_{\text{p.p.}}(\infty)$, based on the moments of the line shape function M_n, is obtained by approximating the integral in Eq. (7) by a Gaussian. We have

$$\Delta H_{\text{p.p.}}(\infty) = (2/\sqrt{3})(\hbar/g\mu_B T_2) = (2\pi/3)^{1/2}(\hbar/g\mu_B)(M_2)^{3/2}/(M_4)^{1/2}. \quad (8)$$

In the following section, we will make use of Eq. (8) to analyze the linewidth in $LaMnO_3$ and $CaMnO_3$.

III. $LaMnO_3$ and $CaMnO_3$

In this section, we analyze the EPR linewidth in both $LaMnO_3$ and $CaMnO_3$. In Fig. 2, we display the linewidth as a function of temperature for $LaMnO_3$ and $LaMnO_{3.04}$. Shown on the graph are the temperatures T_{JT} associated with the Jahn-Teller (JT) transition from the low-temperature orthorhombic O′ to the high-temperature pseudo cubic O phase. By excluding data near the antiferromagnetic transition, where the linewidth diverges, and just below the Jahn-Teller transition, where the linewidth decreases, one can infer values of $\Delta H_{\text{p.p.}}(\infty)$. In the case of $LaMnO_3$, we have $\Delta H_{\text{p.p.}}(\infty) = 3100$ and 2600 G for the O′ and O phases, respectively.[10] In contrast, in the case of $LaMnO_{3.04}$, $\Delta H_{\text{p.p.}}(\infty)$ is approximately the same for both phases and similar to the value found for the O phase in $LaMnO_3$.

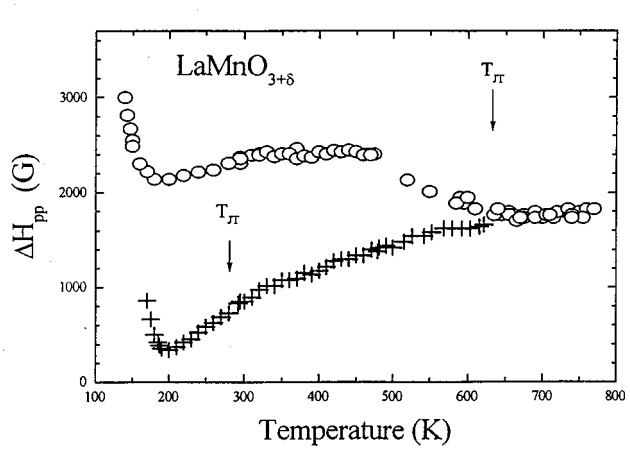

FIG. 2. Linewidth of $LaMnO_{3+\delta}$ for $\delta = 0$ (○) and 0.04 (+). Jahn-Teller transition temperatures between the O′ and O phases are indicated.

A. Calculation of the moments

Our analysis is based on a calculation of the spectral moments M_n appearing in the expression for $\Delta H_{\text{p.p.}}(\infty)$ displayed in Eq. (8). As noted elsewhere,[11] the dipolar interaction contributes only a few gauss to the linewidth. As a result, it is necessary to analyze other contributions, particularly those expected to be sensitive to the structural changes; as discussed in Ref. 10, these are the crystal field and antisymmetric exchange interactions. In the following, we present the expressions for M_2 and M_4 for both interactions.

1. Crystal field

The noncubic component of the crystal field interaction between a Mn ion and its oxygen neighbors can be represented by the second-order effective Hamiltonian

$$H_{\text{CF}} = -DS_z^2 + E(S_x^2 - S_y^2). \quad (9)$$

In the quasicubic local environment of the Mn ions found in the orthorhombic structure of $La_{2/3}Mn_{1/3}O_3$ and the high-temperature O phase of $LaMnO_{3+\delta}$, H_{CF} is expected to be small, so we take $D = E = 0$. In the case of the Jahn-Teller-distorted structure of $LaMnO_{3+\delta}$ (O′ phase), a simplified picture follows by taking $E = 0$, which is strictly valid when the oxygen octahedra have C_{4v} symmetry, i.e., elongated with $l > m = s$ or oblate with $l = m > s$, where l,m, and s refer to the long, medium, and short Mn-O distances, respectively. The distortion in the O′ phase can be characterized by a series of octahedra elongated alternately along the a and c axes (orbital ordering).[12] In this case, the total Hamiltonian may be written as

$$H_{\text{CF}} = -D\sum_{i=1}^{N/2} S_{x(i)}^2 - D\sum_{j=1}^{N/2} S_{z(j)}^2, \quad (10)$$

where the indices i and j represent alternate sites in the (ac) planes. Here we follow the notation of Ref. 13 for the *Pnma* structure.

We have calculated M_2 and M_4 assuming an isotropic Heisenberg exchange interaction between Mn ions on sites k and l, i.e., $H_{ex}=-2\Sigma_{kl}J_{kl}\mathbf{S}_k\cdot\mathbf{S}_l$. In general, we may distinguish two different exchange constants: J_{ac} describing the nearest-neighbor interaction within the ac plane and J_b, the interplane nearest-neighbor interaction. The expressions obtained are dependent on the relative orientation of the radio-frequency field $\mathbf{h}_1$, with respect to the crystal axes. Both moments are isotropic when $\mathbf{h}_1$ is in the (ac) plane, and the angular variation when $\mathbf{h}_1$ has a component along the b axis is given by

$$M_2=(4S^2+4S-3)D^2(1+\cos^2\theta)/10, \tag{11a}$$

$$M_4=(24/5)S(S+1)(4S^2+4S-3)(1+\cos^2\theta)\langle J^2\rangle, \tag{11b}$$

where $\langle J^2\rangle=(2J_{ac}^2+J_b^2)/3$ and θ is the angle between $\mathbf{h}_1$ and the b axis. For a powder sample, we assume an average value $\langle 1+\cos^2\theta\rangle=4/3$.

2. Antisymmetric exchange (Dzialozhinsky-Moriya interaction)

Antisymmetric contributions to the superexchange interaction between Mn ions are allowed when the oxygen ions that mediate the interaction occupy crystal sites that lack inversion symmetry.[14,15] The tilting of the oxygen octahedra present in most perovskites shifts the apical oxygen away from the [010] axis, thus giving rise to a Dzialozhinsky-Moriya (DM) coupling between the (ac) planes. The JT distortions within the (ac) planes give rise to additional contributions to the DM coupling in the O′ phase of $LaMnO_{3+\delta}$. A general Hamiltonian for this interaction is

$$H_{DM}=\sum_{j<k}\mathbf{D}_{DMjk}\cdot(\mathbf{S}_j\times\mathbf{S}_k). \tag{12}$$

Following the calculations of Castner and Seehra,[16] we derived expressions appropriate to the *Pnma* structure of our samples. For a homogeneous powder, we obtained

$$M_2=(2/9)S(S+1)[4(D_{DMx}^2+D_{DMy}^2+D_{DMz}^2)+2(D_{DM'x}^2+D_{DM'z}^2)], \tag{13a}$$

$$M_4=(4/81)S^2(S+1)^2[P(D_{DMx}^2+D_{DMy}^2)+QD_{DMz}^2+R(D_{DM'x}^2+D_{DM'z}^2)+VD_{DMx}D_{DM'x}], \tag{13b}$$

where D_{DMx}, D_{DMy}, and D_{DMz} refer to the components of the intraplane interactions, $D_{DM'x}$ and $D_{DM'z}$ to the interplane interactions, and

$$P=98J_{ac}^2+12J_b^2+8J_{ac}J_b,$$

$$Q=82J_{ac}^2+12J_b^2+8J_{ac}J_b,$$

$$R=12J_{ac}^2+35J_b^2+8J_{ac}J_b,$$

$$V=8J_{ac}^2+8J_b^2.$$

Solovyev *et al.*[17] have made theoretical estimates of the contributions to $\mathbf{D}_{DMjk}$. Although different, all the values obtained had the same order of magnitude. Thus, without losing generality, we may assume a common magnitude $D_{DM}=|D_{DM}|$ for all of them. In this case, the moments are given by

$$M_2\approx 16[(2/9)S(S+1)]D_{DM}^2, \tag{14a}$$

$$M_4\approx 464[(2/9)S(S+1)]^2D_{DM}^2\langle\langle J^2\rangle\rangle, \tag{14b}$$

where $\langle\langle J^2\rangle\rangle=(310J_{ac}^2+114J_b^2+40J_{ac}J_b)/464$.

B. Data analysis

We have analyzed the $\Delta H_{p.p.}(\infty)$ data for $LaMnO_3$ and $CaMnO_3$ displayed in Table I and have compared our values with the results of moment calculations based on experimental values for the isotropic exchange interactions and estimates for the crystal field and DM parameters.

For $LaMnO_3$, all Mn ions are in a trivalent state and $S=2$. Using Eq. (8), one obtains the result

$$g\mu_B\Delta H_{p.p.}(\infty)=(2\pi/3)^{1/2}(2.8D^2+21.3D_{DM}^2)^{3/2}/(806.4D^2\langle J^2\rangle+824.9D_{DM}^2\langle\langle J^2\rangle\rangle)^{1/2}, \tag{15}$$

assuming additivity of the contributions to the moments from the crystal field and DM interactions. As noted in Table I, $\Delta H_{p.p.}(\infty)=3100$ and 2600 G have been reported for the O′ and O phases, respectively.[10] Likewise, sets of values for J_{ac} and J_b have also been determined. Above T_{JT} (O phase), $LaMnO_3$ has ferromagnetic nearest-neighbor interactions with $J_{ac}=J_b=9.6$ K. Below T_{JT} (O′ phase), the interplane exchange becomes antiferromagnetic and $J_{ac}=6.6$ K and $J_b=-4.4$ K. From a neutron-scattering experiment at 4.2 K, Moussa *et al.*[18] have inferred the value $D=1.92$ K for the O′ phase. As mentioned, we may assume $D\approx 0$ for the O phase, where the Mn-O distances are approximately equal.[19] Using Eq. (15), we may then derive values for D_{DM}. We obtain $D_{DM}=0.73$ K for $T<T_{JT}$ and $D_{DM}=0.82$ K for $T>T_{JT}$. These results suggest that the antisymmetric exchange remains essentially constant through the JT transition. This behavior is compatible with the origin of the interactions being the tilting of the octahedra, which has been found to be present in both phases [$\varphi=15.2°$ at 573 K and $\varphi=13.6°$ at 798 K (Ref. 19)].

For $CaMnO_3$, the symmetry is also *Pnma* with very little distortion of the oxygen octahedra and a tilting angle[20] $\varphi=13.6°$ at 300 K, similar to the values found in $LaMnO_3$. We may then compare the measured linewidth[21] $\Delta H_{p.p.}(\infty)=1050$ G with that obtained for $LaMnO_3$ in the pseudocubic O phase. If we assume the same value of D_{DM} in both compounds and neglect any contribution from the crystal field interaction in $CaMnO_3$, the ratio of the linewidths is given by

$$\Delta H_{p.p.}(\infty)_{CMO}/\Delta H_{p.p.}(\infty)_{LMO}=0.79|J_{LMO}/J_{CMO}|, \tag{16}$$

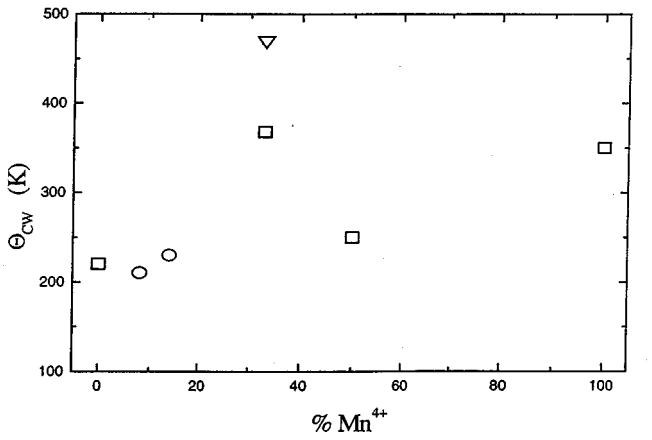

FIG. 3. Θ_{CW} vs % Mn^{4+} content for various manganite compounds: (□) $La_{1-x}Ca_xMnO_3$, (▽) $La_{0.77}Sr_{0.33}MnO_3$, and (○) $LaMnO_{3+\delta}$. In the case of $LaMnO_3$, the linewidth refers to the high-temperature O phase.

where the coefficient 0.79 arises from the different spin value for Mn^{4+} ($S=3/2$).

$CaMnO_3$ orders as a G-type antiferromagnet[22] at $T_N = 125$ K. The Curie-Weiss temperature, determined using the data from Ref. 23, corrected for the Van Vleck contribution to the susceptibility,[24] is $\Theta_{CW} \approx 350$ K. The difference between Θ_{CW} and T_N suggests that second-neighbor interactions need to be taken into account as in the case of $LaMnO_3$.[17] In a mean-field approximation, we derived $J^{(1)} = -16(2)$ K and $J^{(2)} = -4(1)$ K for nearest and second neighbors, respectively. Using this value of $J^{(1)}$ for J_{CMO} in Eq. (16), we obtained a ratio of 0.47, in excellent agreement with the experimental ratio 0.40.

IV. $La_{1-x}Ca_xMnO_3$: $0<x<1$

As shown in Fig. 1, $\Delta H_{p.p.}(\infty)$ for $La_{1-x}Ca_xMnO_3$ decreases with increasing calcium (i.e., Mn^{4+}) concentration. The behavior of $\Delta H_{p.p.}(\infty)$ in the intermediate region $0<x<1$ is in contrast to the variation of the Curie-Weiss (or paramagnetic Curie) temperature Θ_{CW}. As is shown in Fig. 3, with data listed in Table I, the Curie-Weiss temperature has a peak in the neighborhood of $x=1/3$, which is the concentration associated with the highest Curie temperature. It is well established that the maxima in Θ_{CW} and the Curie temperature are a consequence of the double-exchange mechanism. The question then arises as to why the double-exchange mechanism does not have a similarly pronounced effect on $\Delta H_{p.p.}(\infty)$.

The most likely explanation for the apparent absence of the influence of the double exchange on $\Delta H_{p.p.}(\infty)$ lies in the nature of the double-exchange mechanism itself. In the paramagnetic phase, the double exchange arises from the hopping of the e_g electron and its associated lattice distortion (or, equivalently, the hopping of the e_g Jahn-Teller polaron[25]) between Mn ions. As is made clear in Eq. (7), $\Delta H_{p.p.}(\infty)$ involves the time integral of the correlation function of $[S^+, H_{anis}]$. If the correlation function decays rapidly in comparison with the time scale for significant charge redistribution, then, to a first approximation, it will be unaffected by double exchange. When this happens, the decay of the correlation function will be determined primarily by the superexchange interaction between the Mn ions.

In the preceding section, we inferred comparable values for the magnitudes of the nearest-neighbor superexchange interactions in $CaMnO_3$(16 K) and in the O phase of $LaMnO_3$ (9.6 K). Using the ''rule of thumb'' approximation that the magnitude of the superexchange interaction between different spin species in the mixed system is the geometric mean of the magnitudes of the superexchange interactions of the two components, we estimate that the magnitude of the Mn^{3+}-Mn^{4+} interaction is approximately 12 K. With these values of the interactions in the second and fourth moments, together with the assumption that the DM interaction does not change significantly with increasing Ca concentration, we obtain a variation in $\Delta H_{p.p.}(\infty)$ that is qualitatively consistent with the data displayed in Fig. 1.

We can use the equations in the Appendix, together with the results of the data analysis in Sec. III, to obtain an estimate of the characteristic time associated with the decay of the correlation function in $\Delta H_{p.p.}(\infty)$. In the Gaussian approximation, the correlation function decays as $\exp[-(M_4/2M_2)t^2]$ so that a measure of the characteristic time is provided by the ratio $(2M_2/M_4)^{1/2}$. Using the values of the moments appropriate to the high-temperature O phase, we obtain the result $(2M_2/M_4)^{1/2} \approx 0.2/J \approx 2\times10^{-13}$ s. As a consequence, we infer that any charge motion over a time interval on the order of 10^{-13} s is not extensive enough to affect the decay of the correlation function.

V. DISCUSSION

There are a number of comments to be made about the analysis of the preceding sections. First, we emphasize that the temperature dependence found for the linewidth, $\Delta H_{p.p.}(T) \approx [\chi_0(T)/\chi(T)]\Delta H_{p.p.}(\infty)$, does not hold in the vicinity of a strongly distortive Jahn-Teller transition or as T approaches a magnetic ordering transition. This is seen explicitly in Fig. 2 for both types of transitions. In the case of the Jahn-Teller transition, the anomalous behavior of the linewidth reflects the decrease in the crystal field anisotropy as T_{JT} is approached from the low-temperature side. Such an interpretation is also consistent with the observation that the oxygenated sample $LaMnO_{3.04}$ shows a much weaker effect. This behavior is explained by the fact that the oxygen octahedra in the O′ phase of $LaMnO_{3.04}$ are less distorted than in the O′ phase of the stoichiometric compound. As a result, the linewidth below T_{JT} is dominated by the contribution from the Dzialozhinsky-Moriya interaction, which remains approximately constant through the transition. The increase in the linewidth in both samples below 200 K is an example of critical broadening.[26] The correlation function appearing in the expression for the linewidth that is displayed in Eq. (6) grows in magnitude and decays more slowly as $T \rightarrow T_N$, the ordering temperature associated with the canted antiferromagnetic state.

It is evident that in analyzing the temperature dependence of the EPR linewidth, one should remove the effects of the thermodynamic factor $[T\chi(T)]^{-1}$ by considering not $\Delta H(T)$ alone, but rather the product $T\chi(T)\Delta H(T)$.[27] If this is not done, one can be led to premature conclusions about

the origin of the linewidth. In the case of the manganites with $x \approx 1/3$, the rapid decrease of the susceptibility above the ordering temperature results in quasilinear behavior in $\Delta H(T)$, a characteristic that was originally interpreted as indicating a spin-phonon mechanism for the linewidth.[28–30]

The analysis of the linewidths in $LaMnO_3$ and $CaMnO_3$ is relatively straightforward in that conventional techniques based on spectral moments can be utilized to calculate $\Delta H_{\text{p.p.}}(\infty)$. The main complication is to sort out the contributions from the crystal field and Dzialozhinsky-Moriya interactions. The same cannot be said for the analysis of the linewidth of $La_{0.67}Ca_{0.33}MnO_3$. Here the surprise is that while the double-exchange mechanism makes a significant contribution to $\chi(T)$, it does not seem to have an important effect on $\Delta H_{\text{p.p.}}(\infty)$. We attributed the apparent lack of an effect to the rapid decay of the correlation function appearing in Eq. (7). According to our interpretation, the distribution of Mn^{3+} and Mn^{4+} ions appears ''frozen'' on the time scale of 10^{-13} s, which characterizes the decay of the correlation function. As a consequence, the spin dynamics is similar to that of a static random mixture of the two types of ions.

It is evident that further studies are needed to test this hypothesis. If feasible, measurements of the EPR linewidth in double-exchange systems that have metalliclike conductivity in the paramagnetic phase could reveal the influence of the charge dynamics on $\Delta H_{\text{p.p.}}(\infty)$ if the change in valence took place on a time scale that was short in comparison with the exchange frequencies associated with the superexchange interaction.

ACKNOWLEDGMENTS

We wish to acknowledge partial support from the National Science Foundation (U.S.) through Grant Nos. NSF-DMR 9705155 and NSF-INT 9802967, from CONICET, Fundacion Antorchas, and Ministerio de Education–FOMEC (Argentina) and from the Graduate School of the University of Wisconsin–Madison.

APPENDIX

In this appendix, we establish the connection between the linewidth calculation outlined in Sec. II and the analysis based on moments of the line shape function.[31,32] The starting point is Eq. (5a). The first step in the calculation is to perform a Taylor series expansion of the integrand, i.e.,

$$\left(\frac{dS^+(t)}{dt},\frac{dS^-(0)}{dt}\right)=\left(\frac{dS^+}{dt},\frac{dS^-}{dt}\right)+\left(\frac{d^2S^+}{dt^2},\frac{dS^-}{dt}\right)t + \frac{1}{2}\left(\frac{d^3S^+}{dt^3},\frac{dS^-}{dt}\right)t^2+\cdots. \quad \text{(A1)}$$

The various terms on the right-hand side of Eq. (A1) are directly related to the moments of the normalized line shape function $f(\omega)$, defined by

$$f(\omega)=\frac{1}{2\pi(S^+,S^-)}\int_{-\infty}^{+\infty} dt\, e^{-i\omega t}(S^+(t),S^-(0)). \quad \text{(A2)}$$

Denoting these moments by M_n, where M_n is expressed as

$$M_n=\int_{-\infty}^{+\infty} d\omega\, \omega^n f(\omega), \quad \text{(A3)}$$

the right-hand side of Eq. (A1) becomes

$$(S^+,S^-)\left[M_2-\frac{t^2}{2}M_4+\frac{t^4}{4!}M_6-\cdots\right], \quad \text{(A4)}$$

where we have made use of the results that the odd moments vanish since the integrand in Eq. (A2) is an even function of t so that f becomes an even function of ω.

A simple approximation is obtained by assuming that the integrand in Eq. (5a) is a Gaussian with a width determined by the ratio M_4/M_2. This approximation is equivalent to approximating the higher moments by their equivalent Gaussian values, i.e., $M_6=3M_4^2/M_2$, etc. After making this approximation, the linewidth becomes

$$1/T_2=\sqrt{\frac{\pi}{2}}(M_2)^{3/2}(M_4)^{-1/2}, \quad \text{(A5)}$$

in agreement with the results of Ref. 32.

[1] C. Zener, Phys. Rev. **81**, 440 (1951); **82**, 403 (1951).
[2] P. W. Anderson and H. Hasegawa, Phys. Rev. **100**, 675 (1955).
[3] A. J. Millis, P. B. Littlewood, and B. I. Shraiman, Phys. Rev. Lett. **74**, 5144 (1995).
[4] A. J. Millis, Phys. Rev. B **53**, 8434 (1996).
[5] A. J. Millis, B. I. Shraiman, and R. Mueller, Phys. Rev. Lett. **77**, 175 (1996).
[6] J. Topfer and J. S. Goodenough, J. Solid State Chem. **130**, 117 (1997).
[7] M. T. Causa *et al.*, Phys. Rev. B **58**, 3233 (1998), and references therein.
[8] D. L. Huber, Phys. Rev. B **12**, 31 (1975).
[9] H. Mori, Prog. Theor. Phys. **33**, 423 (1965). See also D. Forster, *Hydrodynamic Fluctuations, Broken Symmetry, and Correlation Functions* (Benjamin, Reading, MA, 1975).
[10] M. T. Causa *et al.*, J. Magn. Magn. Mater. **196-197**, 506 (1999).
[11] D. L. Huber, J. Appl. Phys. **83**, 6949 (1998).
[12] J. B. Goodenough, *Magnetism and the Chemical Bond* (Interscience, New York, 1963).
[13] Q. Huang *et al.*, Phys. Rev. B **55**, 14 987 (1997). See also J. B. A. A. Elemans *et al.*, J. Solid State Chem. **3**, 238 (1971). The notation in these references is different from that used by J. Rodríquez-Carvajal *et al.*, Phys. Rev. B **57**, R3189 (1998).
[14] I. Dzialoshinsky, J. Phys. Chem. Solids **4**, 241 (1958).
[15] T. Moriya, Phys. Rev. Lett. **4**, 228 (1960); Phys. Rev. **120**, 91 (1960).
[16] T. G. Castner and M. S. Seehra, Phys. Rev. B **4**, 38 (1971).
[17] I. Solovyev *et al.*, Phys. Rev. Lett. **76**, 4825 (1996).
[18] F. Moussa, M. Hennion, J. Rodríquez-Carvajal, and H. Moudden, Phys. Rev. B **54**, 15 149 (1996).

[19] Rodríquez-Carvajal *et al.* (Ref. 13).
[20] K. R. Poppelmeier, M. E. Leonowicz, J. C. Scanlon, and J. M. Longo, J. Solid State Chem. **45**, 71 (1982).
[21] M. T. Causa *et al.*, J. Phys. IV **7**, C1-355 (1997).
[22] E. O. Wollan and W. C. Kohler, Phys. Rev. **100**, 545 (1955).
[23] J. Briático *et al.*, Phys. Rev. B **53**, 14 020 (1996).
[24] The Van Vleck contribution to the susceptibility was derived following M. E. Lines, Phys. Rev. **164**, 736 (1967), and using the value of 24 000 cm^{-1} for the energy of the first excited state of Mn^{4+}, as given by K. A. Muller, Phys. Rev. Lett. **2**, 341 (1959).
[25] G.-m. Zhao *et al.*, Nature (London) **381**, 676 (1996).
[26] D. L. Huber, Phys. Rev. B **6**, 3180 (1972), and references therein.
[27] M. Tovar *et al.*, J. Appl. Phys. **83**, 7201 (1998).
[28] A. Shengelaya *et al.*, Phys. Rev. Lett. **77**, 5296 (1996).
[29] M. S. Seehra *et al.*, J. Phys.: Condens. Matter **8**, 11 283 (1996).
[30] C. Rettori *et al.*, Phys. Rev. B **55**, 3083 (1997).
[31] J. H. Van Vleck, Phys. Rev. **74**, 1168 (1948).
[32] A. Abragam, *The Principles of Nuclear Magnetism* (Clarendon, Oxford, 1961), pp. 435–440.